Available online at www.sciencedirect.com

ScienceDirect

Energy Procedia 67 (2015) 64 – 69

Energy Procedia

5th Workshop on Metallization for Crystalline Silicon Solar Cells

Determination of the contact resistivity of screen-printed Al contacts formed by laser contact opening

Christopher Kranz[a,*], Bianca Lim[a], Ulrike Baumann[a], Thorsten Dullweber[a]

[a]*Institute for Solar Energy Research Hamelin (ISFH), Am Ohrberg 1, D-31860 Emmerthal, Germany*

Abstract

Next-generation industrial PERC solar cells typically include local laser contact opening (LCO) of a dielectric passivation layer stack at the rear side and subsequent full-area aluminum screen printing and firing. In this work we carry out a variation of the rear contact pitch of *p*-type passivated emitter and rear (*p*-PERC) solar cells to determine the specific contact resistivity of the resulting line-shaped aluminium rear contacts to $\rho_c < 5$ mΩ cm^2. We also use the transmission line method (TLM) to measure ρ_c on PERC-like test wafers and obtain a median value of 3 mΩ cm^2. The determined ρ_c values below 5 mΩ cm^2 confirm recent similar studies and contradict a former publication. The main reason for the discrepancy between the literature values is an inaccurate modelling of the bulk spreading resistance contribution to the total series resistance of PERC solar cells.

Peer-review under the responsibility of Gunnar Schubert, Guy Beaucarne and Jaap Hoornstra

Keywords: Screen-printing; PERC solar cells, contact resistivity

1. Introduction

The vast majority of commercial silicon solar cells currently apply a full-area screen-printed aluminum (Al) rear side contacting the *p*-type silicon wafer. Due to the efficiency limitations caused by a high surface recombination velocity and a low internal reflectance at the rear side, cell manufacturers currently introduce passivated emitter and rear cells (PERC) [1, 2], which feature a dielectric passivation layer stack on the rear and only local Al rear contacts (see Fig. 1a). These rear contacts are typically formed by laser contact opening (LCO) of the passivation layer stack

* Corresponding author. Tel.: +49(0)5151-999 643; fax: +49(0)5151-999 400.
E-mail address: kranz@isfh.de

Peer-review under the responsibility of Gunnar Schubert, Guy Beaucarne and Jaap Hoornstra
doi:10.1016/j.egypro.2015.03.288

and subsequent full-area aluminum screen printing and firing. As manufacturers improve the aluminum pastes to form contacts with low surface recombination even for narrow LCOs the fraction of metallized area at the rear might further decrease in the future, possibly making the series resistance contribution of the contact resistance of the aluminum-silicon interface a noticeable power loss mechanism. Therefore knowledge of the specific contact resistivity ρ_c is required. Gatz et al. [3] used a variation of the rear contact pitch of PERC solar cells to determine ρ_c to 40 – 55 mΩ cm^2. However, for this approach the contribution of the bulk to the series resistance R_b needs to be acquired either by calculation or numerical simulation. Müller et al. [4] showed that the calculation of R_b according to the model of Plagwitz [5] as used in Ref. 3 leads to an underestimation of R_b und thus an overestimation of ρ_c. In this study we apply the method of rear contact pitch variation for *p*-type PERC cells using R_b values acquired by simulation with Sentaurus Device. In addition we manufacture PERC-like test wafers as shown in Fig. 1b) to determine ρ_c using the transmission line method (TLM). We compare the resulting values for ρ_c with those of back-junction *n*-type passivated emitter rear totally diffused solar cells (BJ *n*-PERT). These solar cells are very similar to the PERC solar cells, the differences being only *n*-Si as base material and a full-area boron diffusion of the rear side (see Fig. 1c). However, due to the alloying of Si and Al during the firing step, the B-doped emitter is actually replaced by an Al-doped p^+ region under the Al contacts. As a result, these Al rear contacts are very similar to those of *p*-PERC solar cells, with the exception of contacting the emitter and not the base. Hence, for BJ *n*-PERT cells the variation of the rear contact pitch does not change the contribution of the bulk to the series resistance, simplifying the contact resistivity analysis.

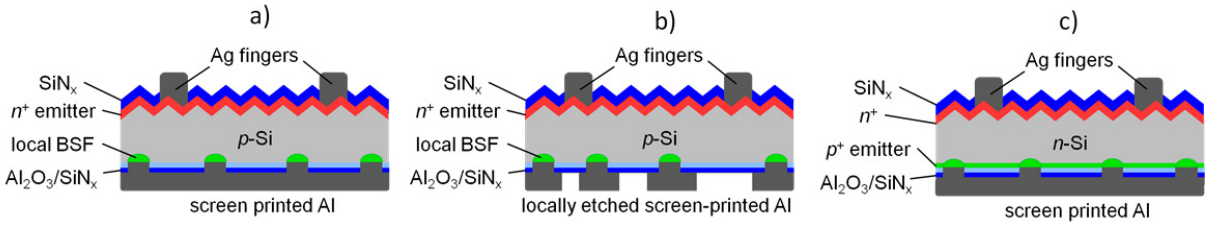

Fig. 1. Schematic drawings of the investigated structures in this paper: a) a *p*-type PERC solar cell; b) a PERC-like TLM sample with isolated rear aluminum contacts; c) an *n*-type PERT back-junction solar cell.

2. Experimental

For the *p*-type PERC solar cells we use 156*156 mm² pseudosquare Czochralski-grown silicon (Cz-Si) with a resistivity of 2 Ω cm. As shown in Table 1 the process flow for the PERC solar cells starts with wafer cleaning and deposition of a dielectric rear protection layer, that allows for subsequent single sided alkaline texturing and a single sided $POCl_3$-diffusion aiming at a sheet resistance of 60 Ω/sq. The phosphorus silicate glass (PSG) and the protection layer are then removed by wet chemistry. After depositing an Al_2O_3/SiN_x passivation layer stack on the rear and a SiN_x antireflection coating (ARC) on the front, we locally ablate the rear passivation layer stack via LCO and subsequently carry out Ag screen-printing on the front and full-area Al screen-printing of the rear. The PERC solar cell process as shown in detail in Ref. 6 then concludes with a co-firing step.

The process for the PERC-like TLM samples is very similar to the one of the PERC solar cells. Until co-firing the only difference is an adapted LCO geometry for different TLM samples on one wafer. Each sample includes different contact line pitches as indicated in Fig 1b). In order to evaluate a dependency of the contact resistivity on the contact line width, there are samples with LCO line widths of 28, 46, 64, 82 and 100 µm. The final contact, that is formed due to the diffusion of the silicon into the aluminum is about 40 µm wider than the LCO line width according to scanning electron microscopy (SEM) cross section images. After firing the contact lines are protected with an etch resistant hot melt wax printed with inkjet and subsequently separated from each other by a KOH Al-etch. After cleaning the different TLM samples are cut out of the wafer.

For the *n*-type PERT back-junction solar cells we use 6 Ω cm P-doped Cz-Si and apply an additional BBr_3 quartz furnace diffusion right after the initial wafer cleaning. The other process steps remain the same, when compared to the *p*-PERC cells (see Tab. 1). Details are described in Ref. 7.

Table 1. Process flows for *p*-type PERC solar cells, PERC-like TLM samples and *n*-type PERT back-junction solar cells.

***p*-PERC**	**TLM samples**	***n*-PERT BJ**
Wafer cleaning	Wafer cleaning	Wafer cleaning
		B-diffusion
Rear protection layer	Rear protection layer	Rear protection layer
Texturing	Texturing	Texturing
P-diffusion	P-diffusion	P-diffusion
PSG + dielectric etch	PSG + dielectric etch	PSG + dielectric etch
Passivation	Passivation	Passivation
Laser contact opening	Laser contact opening	Laser contact opening
Screen-printing	Screen-printing	Screen-printing
Co-firing	Co-firing	Co-firing
	Inkjet etch resistant	
	Al-etch	
	Cleaning + laser cutting	

3. Results and Discussion

3.1. Determination of ρ_c by varying the pitch of PERC solar cells

We vary the rear contact pitch p of PERC solar cells and measure the series resistance R_s in dependence of the inverse metallization fraction $1/f$ according to

$$R_s - R_b = \rho_c \cdot \frac{1}{f} + R_{const} \quad , \tag{1}$$

where R_{const} are the series resistance contributions that do not depend on the rear side metallization fraction (e.g. the front Ag finger grid). We need to acquire the series resistance of the bulk R_b in order to determine the contact resistivity ρ_c. Using a triple-light-level [8] simulation with Sentaurus device, we obtain the R_b values at the maximum power point of the solar cell as shown in Fig. 2. The used simulation domain includes a fully contacted front side and therefore neglects the resistance contributions caused by lateral current flows through the emitter. However, this approach allows us to freely choose the rear contact pitch and keep the simulation domain at a manageable size.
Fig. 2 also compares the values obtained by simulation with those calculated according to the analytical model of Plagwitz [3], which is based on the calculation of the spreading resistance introduced by Gelmont et al. [9]. At pitches larger than 1500 µm the simulated values strongly exceed the calculated values according to Plagwitz, which were used in the analysis of Gatz et al. [3]. The values calculated according to another analytical model introduced by Saint-Cast [10] almost match the simulated values.

A fit to the original data from Ref. 3, which includes R_b values according to the model of Plagwitz, strongly overestimates the specific contact resistivity ρ_c = (55 ± 5) mΩ cm² as shown in Fig. 3a). Application of the numerically obtained values for R_b to equation (1) leads to a correction of this data with R_s-R_b values following no clear trend. However, the corresponding fit results in ρ_c = (-9 ± 12) mΩ cm², indicating a smaller value of ρ_c. Fig 3a) also shows that evaluation with the Plagwitz model is only valid for small values of $1/f < 10$. A linear fit to the contact pitch variation of this work yields a contact resistivity of ρ_c = (-0.9 ± 1.1) mΩ cm² as shown in Fig. 3b). Since the stated value for the uncertainty of ρ_c only accounts for the scattering of the data, we find a line with maximum slope within the error bars of all data points to derive an upper limit of $\rho_c < 5$ mΩ cm².

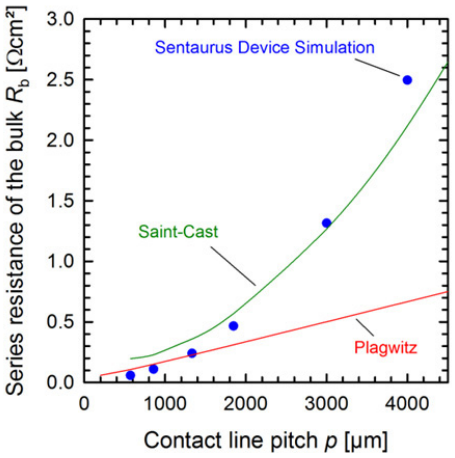

Fig. 2. Contribution of the silicon bulk to the total series resistance R_b in dependence of the contact line pitch as determined by Sentaurus Device simulation (blue), the model of Plagwitz (red) and the model of Saint-Cast (green).

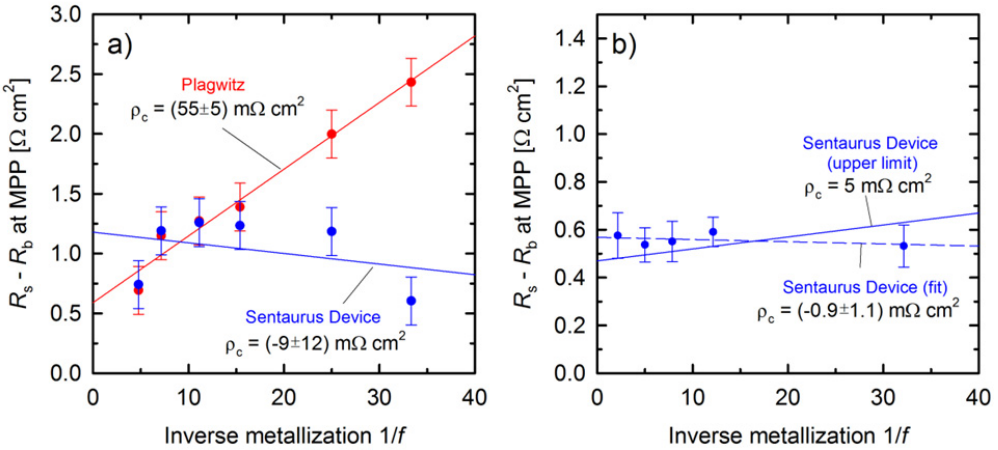

Fig. 3. R_s-R_b vs. inverse metallization fraction 1/f: Values resulting from a calculation of R_b with the model of Plagwitz are red, whereas values including an R_b obtained by simulation with Sentaurus device are blue. a) shows the original data from Ref. 3, b) shows the data of this work.

3.2. Determination of ρ_c by TLM measurements

In addition to the measurement at PERC solar cells we measure the contact resistivity ρ_c in dependence of the contact line width applying the standard TLM at samples as shown in Fig. 1b). Since the standard TLM evaluation assumes a thin conductive layer instead of a bulk of finite thickness, we expect our measurements to overestimate the actual contact resistivity. An advanced evaluation that accounts for this bulk contribution has recently been introduced [11], but is however not yet applied to our measurements. The results for ρ_c (see Fig. 4) show a trend towards larger scattering for narrower contact lines, which is probably due to the fact that the uncertainty of the contact line width translates into a relatively larger uncertainty of the area of the aluminum-silicon interface. Furthermore we observe differences of the median values of the distributions for ρ_c when moving from one tested contact line width to the next. However, these shifts do not show any systematic behaviour, in contrast to the data reported by Urrejola et al. [12], who observed an increase of ρ_c from around 9 mΩ cm² to 17 mΩ cm² when moving from an LCO width of 80 µm to 170 µm. With the median values for the single line widths being around or smaller

than 5 mΩ cm² and an overall median value of 3 mΩ cm² the estimation $\rho_c < 5$ mΩ cm² as derived from our solar cell analysis remains valid.

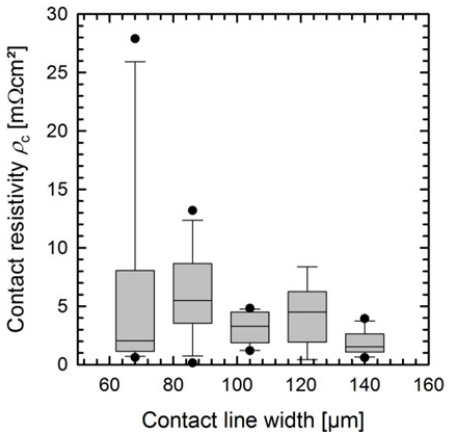

Fig. 4. Specific contact resistivity ρ_c in dependence of the contact line width after firing as measured with the transmission line method (TLM). The plot shows a total of 61 measurements with 9-16 measurements per contact line width.

3.3. Determination of ρ_c by varying the pitch of n-PERT back-junction solar cells

We also apply a rear contact pitch variation to our *n*-type PERT BJ solar cells and measure the series resistance R_s using the double-light-level method. Apart from the contact resistance the only pitch dependent contribution to R_s is the contribution of the emitter R_{em}. Hence, R_b in equation (1) is substituted by R_{em} when analyzing PERT BJ cells instead of PERC cells. All other series resistance contributions are again assumed to be independent of the rear contact pitch. The series resistance contribution of the emitter R_{em} is obtained by two-dimensional simulations using the conductive boundary (CoBo) model [13] and Quokka software [14]. Fig. 5 shows that a linear fit to the resulting values for R_s-R_{em} yields a contact resistivity of (8 ± 2) mΩ cm² as published in more detail in Ref. 7, which is slightly higher than the determined value of our *p*-type PERC cells, but again by almost one order of magnitude smaller than the 40 – 55 mΩ cm^2 reported in Ref. 3.

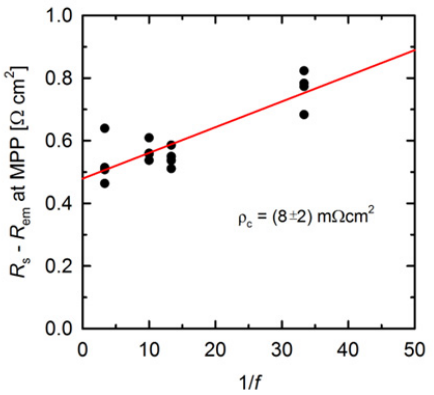

Fig. 5. R_s-R_{em} vs. inverse metallization fraction 1/*f* for the *n*-type PERT BJ solar cells. Figure taken from Ref. 7.

4. Conclusion

We processed *p*-type PERC solar cells and PERC-like TLM samples in order to measure the specific contact resistivity ρ_c of line-shaped screen-printed Al contacts via contact pitch variation and TLM, respectively. A fit to the solar cell data yielded a small value of $\rho_c = (-0.9 \pm 1.1)$ mΩ cm^2, whereas the TLM measurements resulted in a median value of $\rho_c = 3$ mΩ cm^2. We therefore derive an upper limit of $\rho_c < 5$ mΩ cm^2. Recently Müller et al. [4] pointed out, that the analysis of the pitch variation in Ref. 3 with a reported value of 40 – 55 mΩcm^2 used an inappropriate model for the calculation of the bulk contribution to the series resistance. According to their findings they state an absolute resistance per line of 0.46 Ωcm, which – using their contact width of 60 µm – corresponds to a contact resistivity of 3 mΩ cm^2 and is in good accordance with our results. Using the upper limit of 5 mΩ cm^2 and a typical metallization fraction of $f = 10\%$ we estimate a small rear contact resistance of $R_c = \rho_c / f = 0.05$ Ω cm^2, which contributes to a total series resistance of $R_s = 0.7$ Ω cm^2. We also carried out an analogous pitch variation for *n*-type PERT back-junction solar cells and obtained $\rho_c = (8 \pm 2)$ mΩ cm^2, which is slightly higher, but still comparable to the result of the PERC cells. The resulting PERC solar cells of this work achieve energy conversion efficiencies up to 21.2% [15, 16] when applying a 5 busbar front grid, whereas the *n*-PERT BJ solar cells demonstrate 20.5% [7] with a conventional 3 busbar layout.

Acknowledgements

We thank our colleagues at ISFH for support in solar cell processing. This work was funded by the German Federal Ministry for the Environment, Nature Conservation and Nuclear Safety (contract number 0325296) and by our industry partners Heraeus Precious Metals, Rena, Singulus Technologies and SolarWorld within the R&D project HighScreen.

References

[1] G. Fischer, K. Strauch, T. Weber et al., Simulation based development of industrial PERC cell production beyond 20.5% efficiency, Energy Procedia, Volume 55, 2014, p. 425–430
[2] J. W. Müller, P. Engelhart, B. Klöter et al., Current status of Q.Cells´ high-efficiency Q.ANTUM technology with new world record module results, Proc. 27th EU PVSEC, p. 661–665 (2012)
[3] S. Gatz, T. Dullweber, and R. Brendel, Evaluation of Series Resistance Losses in Screen-Printed Solar Cells With Local Rear Contacts, Photovoltaics, IEEE Journal of , vol.1, no.1, pp.37,42, July 2011
[4] M. Müller, and F. Lottspeich, Evaluation of determination methods of the Si/Al contact resistance of screen-printed passivated emitter and rear solar cells, Journal of Applied Physics, 115, 084505 (2014)
[5] H. Plagwitz, Ph.D. thesis, University of Hannover, Faculty of Mathematics and Physics, Hannover, 2007
[6] T. Dullweber et al., Towards 20% efficient large-area screen-printed rear-passivated silicon solar cells, Prog. Photovolt. 20(6); 2012, p. 630–638
[7] B. Lim et al., n-PERT back junction solar cells: an option for the next industrial technology generation?, 29th EU PVSEC, 2014, in press
[8] K. C. Fong, K. R. McIntosh, and A.W. Blakers, Accurate series resistance measurements of solar cells, Prog. Photovolt: Res. Appl. 2013; 21:490–499
[9] B. Gelmont, M. S. Shur, and R. J. Mattauch, Solid-State Electronics 38(3), 731–734 (1995)
[10] P. Saint-Cast, Ph.D. thesis, University of Konstanz, Department of Physics, Konstanz, 2012
[11] S. Eidelloth and R. Brendel, Analytical theory for extracting specific contact resistances of thick samples from the transmission line method, IEEE Electron Device Letters 35 (1), pp. 31–43 (2014)
[12] E. Urrejola, K. Peter, H. Plagwitz et al., Al-Si alloy formation in narrow p-type Si contact areas for rear passivated solar cells, J. Appl. Phys. 107, 124516 (2010)
[13] R. Brendel, Prog. Photovolt: Res. Appl. 20, pp. 31–43 (2012)
[14] A. Fell, IEEE Trans. Electron Devices 60 (2), pp. 733–738 (2012)
[15] H. Hannebauer, T. Dullweber, U. Baumann et al., (2014), 21.2%-efficient fineline-printed PERC solar cell with 5 busbar front grid. Phys. Status Solidi RRL, 8: 675–679.
[16] T. Dullweber et al., Fine-line printed 5 busbar PERC solar cells with conversion efficiencies beyond 21%, 29th EU PVSEC, 2014, in press